Preparation, isolation, storage, and spectroscopic characterization of water vapor enriched in the ortho-H_2O nuclear spin isomer

Pierre-Alexandre Turgeon,[1] Patrick Ayotte,[1,*] Elina Lisitsin,[2] Yossi Meir,[2] Tatyana Kravchuk,[2] and Gil Alexandrowicz[2,†]

[1]*Département de Chimie, Université de Sherbrooke, 2500 Boulevard Université, Sherbrooke, Québec, Canada J1K 2R1*

[2]*Schulich Faculty of Chemistry, Technion-Israel Institute of Technology, Technion City, Haïfa 32000, Israel*

(Received 14 September 2012; published 21 December 2012)

Using magnetic focusing in a supersonic jet, a beam of "normal" H_2O molecules seeded in a krypton carrier gas is shown to provide a source of water molecules that is highly enhanced in the ortho-H_2O (o-H_2O) nuclear spin isomer over the high-temperature equilibrium 3:1 ortho:para ratio. Water from the magnetically focused beam is then isolated and stored within a Kr matrix at 13 K whereby the amplitude and lifetime of this strong nuclear spin polarization are quantified spectroscopically. Attempts to store the polarization in a colder Kr matrix reveal complex nuclear spin conversion processes.

DOI: 10.1103/PhysRevA.86.062710 PACS number(s): 34.90.+q, 33.15.Kr, 37.20.+j

I. INTRODUCTION

Strategies to separate nuclear spin isomers have been devised ever since they were predicted to exist [1,2], and soon thereafter discovered [3,4]. Efficient heterogeneous catalytic conversion methods for the preparation of para-hydrogen (p-H_2) samples enabled rigorous investigations of their physical properties [5]. In comparison, things unfortunately look rather bleak for most polyatomic molecules as their low vapor pressure and comparatively facile interconversion conspire to render their enrichment through heterogeneous catalysis inapplicable. Accordingly, most enrichment techniques for polyatomic molecules rely on manipulations in the gas phase [6–10]. Unfortunately, these methods remain so far impractical to generate even an ever so slight out-of-equilibrium distribution in water vapor. Efficient separation of the nuclear spin isomers of H_2O would facilitate studies of the mechanism and rates by which they interconvert, issues of particular relevance to the origin of icy bodies in the interstellar medium (ISM) [11,12]. Another incentive resides in the potential for novel applications, by analogy with the significant enhancement in the sensitivity of NMR achieved using p-H_2 [13].

Over a decade ago, Tikhonov and Volkov [14] achieved a potential breakthrough by demonstrating the separation of the nuclear spin isomers of H_2O by selective physical adsorption and reporting the preparation of water and ice samples with an o-H_2O:p-H_2O ratio (OPR) $\geqslant$10. To this day however, this approach [14] remains highly controversial mainly due to the inability to reproduce these results [15,16] but also due to the surprisingly long nuclear spin conversion (NSC) times reported for the liquid (i.e., 26–55 min) and solid (i.e., at least a few months) phases of water [17,18]. Alternatively, some of us recently demonstrated [19] that a molecular beam of water can be magnetically focused, leading to an enhancement in its o-H_2O content.

One's ability to separate nuclear spin isomers and the lifetime of enriched samples are both dictated by the rates of NSC. For isolated H_2O molecules, it has mostly been assumed that NSC is so inefficient that it can safely be neglected over most laboratory time scales. However, intermolecular collisions can trigger NSC in the gas phase as described by the so-called quantum relaxation model (QRM) [6,20]. Using this model to study o-$H_2O \leftrightarrow p$-H_2O interconversion in water vapor [15,16,20], NSC rates reaching a maximum value near 0.8 s^{-1} at 20 Torr and 296 K were recently reported [16]. Obviously, such high rates impose stringent constraints to enrichment methods as well as to storage strategies. However, QRM also predicted NSC rates to decrease steeply with decreasing temperature and pressure [16], supporting claims that this "memory" of the H_2O molecule spin states could be preserved over astronomical time scales under the cold and rarefied conditions of the ISM [11,12].

Interestingly, matrix isolation spectroscopy (MIS) [21–24] presents the cold, inert, and rarefied conditions required for isolation, storage, and characterization of water samples highly enriched in o-H_2O. Indeed, the gaslike quasifree rotations of highly diluted H_2O molecules are preserved in substitutional sites of rare-gas (Rg) matrices (i.e., H_2O @ Rg) [21–24]. Furthermore, spin states' populations can thus be straightforwardly interrogated using rovibrational spectroscopy. Indeed, detailed MIS studies of NSC in H_2O@Rg at 4.2 K and high dilution ratios have reported conversion half-times greater than 5 h. NSC rates in H_2O@Rg increase strongly with temperature [25,26] and vary with the chemical nature of the matrix [21,25–29], suggesting a different mechanism than in the gas phase that involves couplings with phonons [21,25]. Finally, evidence for an intermolecular homonuclear dipolar magnetic coupling mechanism has also been unveiled by observations of increasing NSC rates with increasing water concentrations in H_2O@Rg [25,27,29], as well as in supersonic jets of H_2O seeded in rare gases [30,31]. This mechanism should allow for even faster NSC in water clusters (e.g., $\sim$100 μs for the water dimer) [17,18] and other condensed phases of water. For example, attempts to prepare p-$H_2O_{(g)}$ by rapid sublimation of a p-H_2O@Ar sample at 4 K resulted in complete conversion back to "normal" water (i.e., OPR$\sim$3) [29]. Globally, these considerations of enhanced NSC rates at elevated temperatures and concentrations, as well as in condensed water phases, have cast strong doubts over the

*patrick.ayotte@usherbrooke.ca
†ga232@tx.technion.ac.il

slow NSC reported for water and ice by Tikhonov and Volkov [14].

II. EXPERIMENTAL METHODS

For this study, we built a unique apparatus which is a combination of a magnetically focused molecular beam source [19] and a MIS setup allowing the preparation, isolation, storage, and characterization of water samples enriched in the *o*-H_2O nuclear spin isomer. Briefly, a molecular beam of water was cooled and inversely seeded in a krypton supersonic expansion (3% H_2O, 400 mbar, 200-μm-diam nozzle). Separation of the *o*-H_2O and *p*-H_2O nuclear spin isomers was performed by passing the resulting beam through a hexapolar magnetic lens as reported previously [19]. The strongly inhomogeneous hexapolar magnetic field (reaching a gradient of $\sim$2000 T/m) [32] caused the *o*-H_2O molecules having the $m_S = +1$ nuclear spin projection to experience a radial restoring force which converged their trajectory to a focal point $\sim$1.5 m downstream onto the beam axis, while those having $m_S = -1$ were defocused. The *o*-H_2O and *p*-H_2O molecules which displayed $m_S = 0$ remained unaffected by the field, and their trajectories diverged following the angular spread of the beam. The focal point of the magnetic hexapole was centered onto a 1.5-mm-diam aperture allowing the portion of the beam most enriched in *o*-H_2O to enter the UHV analysis chamber.

At the center of the UHV analysis chamber, the $\sim$30:1 Kr:H_2O molecular beam impinged onto a mechanically polished copper block maintained at a low temperature by a closed-cycle helium cryostat where it condensed, forming a binary solid film. The temperature of the substrate was measured using a calibrated silicon diode and was controlled by resistive heating. In order to reach the desired dilution ratio (i.e., >500:1, Kr:H_2O), additional Kr gas was simultaneously condensed onto the substrate by backfilling the UHV chamber ($P_{Kr} = 10^{-5}$ mbar). While trace amounts of $H_2{}^{16}O$ water were mixed with the Kr gas supplied to grow the matrix by background deposition, isotopically labeled $H_2{}^{18}O$ was used in the molecular beam allowing them to be distinguished spectroscopically. The relative abundance of $H_2{}^{16}O$ and $H_2{}^{18}O$ in the matrix could thus be controlled simply by adjusting the backfilling pressure with respect to the constant magnetically focused molecular beam flux. The background-deposited $H_2{}^{16}O$ vapor was assumed to have thermalized with the vacuum chamber walls at 300 K prior to condensing onto the substrate (i.e., referred to as "normal" water and characterized by an OPR = 3) thereby providing an internal standard with which properties of the magnetically focused beam-deposited $H_2{}^{18}O$ could be compared and contrasted.

The OPR of H_2O@Kr was determined by analyzing the rovibrational fine structure monitored by MIS [21,24–29]. Briefly, the unpolarized infrared beam was focused onto the copper substrate and the diverging beam reflected from the substrate was refocused onto a liquid nitrogen cooled 1-mm^2 HgCdTe detector. The optical path external to the UHV chamber was purged from atmospheric contamination. MIS spectra were coaveraged for 400 scans ($\sim$5 min) at 1 cm^{-1} resolution [i.e., $I(\omega)$]. They are reported as absorbance spectra, $\mathcal{A} = -\log[I(\omega)/I_o(\omega)]$, using the bare substrate reflectivity as reference [i.e., $I_o(\omega)$].

III. RESULTS AND DISCUSSION

The expanded view of the water bending range of a typical MIS spectrum (i.e., 1550–1650 cm^{-1}) displayed in Fig. 1 reveals the four rovibrational bands that are by far the most intense spectral features for a dilute H_2O@Kr sample at 13 K composed of a mixture of background-deposited $H_2{}^{16}O$ (labeled in red) and magnetically focused beam-deposited $H_2{}^{18}O$ (labeled in blue). The peaks located at 1605.8 and 1620.9 cm^{-1} were assigned previously to the $1_{01}\rightarrow 1_{10}$ (i.e., *o*-H_2O) and $0_{00}\rightarrow 1_{11}$ (i.e., *p*-H_2O) rovibrational transitions of $H_2{}^{16}O$@Kr, respectively [21,24–29]. Those located at 1598.8 cm^{-1} (i.e., *o*-H_2O) and 1613.1 cm^{-1} (i.e., *p*-H_2O) are assigned herein to the corresponding rovibrational transitions of $H_2{}^{18}O$@Kr, in accordance with the isotopic shift measured in the gas phase [33–35], as well as in neon and argon matrices [22–24].

At 13 K, more than 95% of all H_2O molecules reside in their rotational ground state, namely the 0_{00} and 1_{01} states for *p*-H_2O and *o*-H_2O, respectively. Therefore, the relative abundance of the *o*-H_2O and *p*-H_2O isomers could be evaluated from the amplitude of the two pairs of transitions using their absolute quantum mechanical transition dipole moment (TDM)

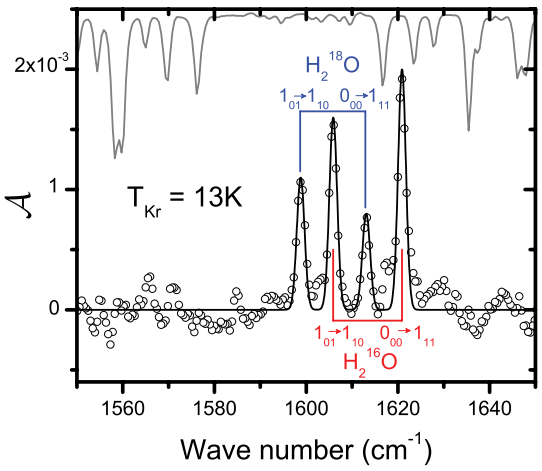

FIG. 1. (Color) Details of the water bending spectral range of a typical MIS spectrum (a line guides the eye through experimental data, ○). The sample was grown by background deposition of $H_2{}^{16}O$ (red labels) and Kr at a substrate temperature of 13 K and a total pressure of 1×10^{-5} mbar for 2134 s at which point concomitant deposition of $H_2{}^{18}O$ (blue labels) from the magnetically focused molecular beam commenced and lasted for 75 min. Beam deposition was delayed to demonstrate the absence of contamination in the spectral region of interest, and of isotopic contamination in the two independent Kr seed gases. In gray scale, a (transmittance) spectrum of water vapor is overlaid showing that fluctuations in the purge gas do not interfere with our measurement. The assignment of the four spectral features to the $0_{00}\rightarrow 1_{11}$ and $1_{01}\rightarrow 1_{10}$ rovibrational bending transitions of *p*-H_2O and *o*-H_2O, respectively, was made according to the literature for $H_2{}^{16}O$@Kr [21,24,25,27] and to isotopic shifts measured in the gas phase [33–35], $H_2{}^{18}O$@Ne [23] and $H_2{}^{18}O$@Ar [22,24].

providing a *spectroscopic* OPR [25,27]. Indeed, the $[1_{01}]/[0_{00}]$ population ratio (i.e., *spectroscopic* OPR = 0.645) is calculated to be only 7% smaller than the equilibrium constant (i.e., *thermodynamic* OPR = 0.694) for $H_2\,{}^{16}O_{(g)}$ at 13 K [33,34]. In water vapor [33–35], H_2O@Ar [28], and H_2O@Ne [25], the TDM for the $1_{01} \rightarrow 1_{10}$ rovibrational bending transition of *o*-H_2O was reported to be a factor (0.49 ± 0.01) smaller than that for the $0_{00} \rightarrow 1_{11}$ rovibrational bending transition of *p*-H_2O. While slightly higher values were reported for H_2O@Kr and H_2O@Xe [25,27], a TDM ratio of 0.5 was used herein, an issue which will be briefly discussed later.

The evolution of the integrated absorbance (corrected for the TDM ratio) of the bands attributed to background-deposited $H_2\,{}^{16}O$ and to magnetically focused beam-deposited $H_2\,{}^{18}O$ through the first 20 000 s of the MIS measurement in Kr at 13 K is displayed in Figs. 2(a) and 2(b), respectively. From this data, the relative abundances of the two nuclear spin isomers of background-deposited water and of magnetically focused beam-deposited water were calculated and are reported in Fig. 2(c). Finally, Fig. 2(d) reports the *spectroscopic* OPR for magnetically focused beam-deposited H_2O (◊) and for background-deposited H_2O (∗) obtained by dividing the relative abundances shown in Fig. 2(c). A vertical line separates data obtained during sample deposition ("Growth") from those where both beam and background deposition were interrupted allowing NSC to be monitored ("Decay").

A few important observations can readily be made from the experimental data: (1) Magnetically focused beam-deposited H_2O displays a substantial enhancement in *o*-H_2O over that carried by background-deposited H_2O. (2) While NSC occurs throughout the experiment with characteristic times on the order of ∼1 h, the OPR of magnetically focused H_2O remains enriched for at least 5000 s over that of "normal" water, for which the highest possible value is OPR = 3. (3) Finally, background-deposited and magnetically focused H_2O converge to an asymptotic value of OPR ∼ 0.7 at long times which is in excellent agreement with the equilibrium spin isomer distributions of $H_2O_{(g)}$ at 13 K [33,34].

Given the slow deposition rates imposed by the molecular beam flux (i.e., $\sim 10^{10}$ H_2O molecules/s), the abundance of the two nuclear spin isomers in magnetically focused water (i.e., blue symbols in Fig. 2) could only be measured reliably ∼10–15 min after beam dosing commenced. Consequently, while a strong enhancement in *o*-H_2O is already noticeable in the first few measurements (OPR > 7; *o*-H_2O relative abundance > 88%), the comparatively rapid NSC suggests that the initial relative abundances and OPR, which could correspond to those in the magnetically focused beam, should display even higher values. To estimate these latter values, extrapolation of the experimental data to the time the beam was turned on (i.e., before NSC in the matrix could alter the initial concentrations) was performed using a simple kinetics model.

The coupled growth and decay kinetics of these experiments was described by two distinct regimes in the model. In the decay portion (i.e., to the right of the vertical line, Fig. 2), NSC coupled the evolution in the nuclear spin isomer populations though simple reversible first-order kinetics [25–28]. Straightforward analysis yielded effective NSC rate constant (i.e., $k_{\text{eff}} = k_{o\rightarrow p} + k_{p\rightarrow o}$, the sum of the elementary NSC rate constants) and final OPR. Zero-order terms were added to the rate equations [36] in order to describe the deposition of *o*-H_2O and *p*-H_2O to the Kr matrix from the magnetically focused beam (i.e., for $H_2\,{}^{18}O$) and from the background (i.e., for $H_2\,{}^{16}O$) during sample growth (i.e., to the left of the vertical line in Fig. 2). As values for the rate constants were determined from analysis of the decay kinetics and equilibrium constants, the growth kinetics model presented a single adjustable parameter namely, the initial OPR.

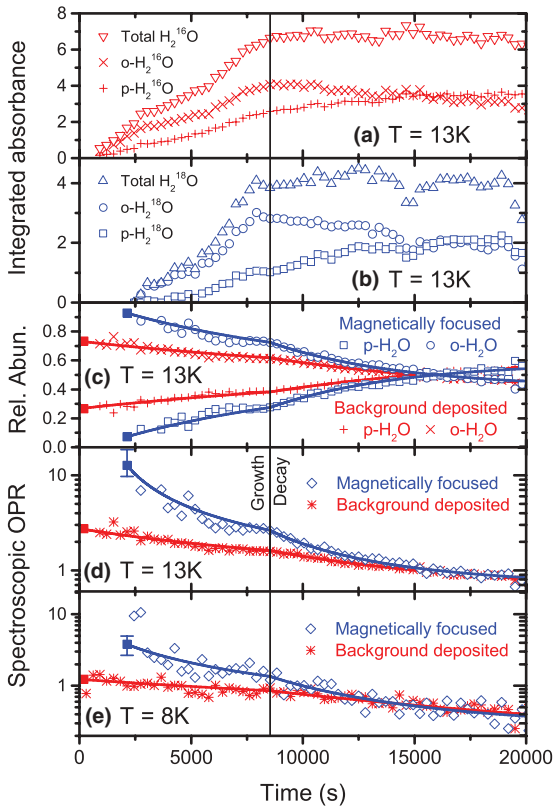

FIG. 2. (Color) The time series in panels (a) and (b) show the integrated absorbance (corrected for the TDM ratio and averaged over five MIS experiments) of the bands attributed to background-deposited water [*p*-$H_2\,{}^{16}O$ (+) and *o*-$H_2\,{}^{16}O$ (×) and their sum (▽)] and to magnetically focused beam-deposited water [panel (b): *p*-$H_2\,{}^{18}O$ (□) and *o*-$H_2\,{}^{18}O$ (○) and their sum (Δ)] in Kr at 13 K, respectively. Panel (c) displays the relative abundances of *p*-H_2O and *o*-H_2O for which experimental uncertainties range from 10% (at short times) to 2.5% as estimated from the standard deviation over five MIS experiments. Panel (d) displays the spectroscopic OPR for background-deposited H_2O (*) and magnetically focused beam-deposited H_2O (◊) in Kr at 13 K. Panel (e) displays the spectroscopic OPR of background-deposited H_2O and magnetically focused beam-deposited H_2O in Kr at 8 K. The vertical line indicates when beam and background deposition were interrupted (i.e., at $t = 8534$ s) whereby NSC slowly drove the nuclear spin isomers populations towards their equilibrium distribution. Results from a simple first-order kinetics model describing the coupled growth and decay kinetics [36], displayed as continuous lines in panels (c)–(e), yielded the effective NCS rate constant, k_{eff}, as well as the initial (displayed by filled red and blue squares) and final relative abundances and OPR of background-deposited $H_2\,{}^{16}O$ and magnetically focused beam-deposited $H_2\,{}^{18}O$.

For background-deposited H_2O, fitting the model (red traces in Fig. 2) yielded initial relative abundances of 0.733(6) and 0.267(6) for *o*-H_2O and *p*-H_2O, respectively and an initial OPR = 2.75(8) which are displayed as filled red squares in Figs. 2(c) and 2(d). The agreement of the initial and final OPRs with those expected [33,34] for $H_2O_{(g)}$ at 300 and 13 K, respectively, give credence to our choice of TDM ratio and to the fact the spin states populations of water molecules are mostly preserved during their condensation within the Kr matrix at 13 K. The model also provided $k_{\text{eff}} = 0.33(3)\ \text{h}^{-1}$ which is consistent with values reported by Pardanaud (i.e., $k_{\text{eff}} = 0.37\ \text{h}^{-1}$ and $0.845\ \text{h}^{-1}$ at 12 and 16 K, respectively) [25].

For magnetically focused beam-deposited H_2O, the model (blue traces in Fig. 2) yielded initial relative abundances of 0.93(2) and 0.07(2) for *o*-H_2O and *p*-H_2O, respectively, and an initial OPR $= 13^{+6}_{-3}$ which are displayed as filled blue squares in Figs. 2(c) and 2(d). An *o*-H_2O purity ~93% can thus be achieved through this magnetic focusing methodology, which represents in excess of *a fourfold enrichment in the o-H_2O nuclear spin isomer and supports the interpretation of the previous spatial focusing measurements* [19].

The ability to produce high-purity *o*-H_2O molecular beams opens up various potential applications and research possibilities such as studies of the sticking and scattering of spin isomers of water on surfaces, an important yet controversial topic [14]. Other future applications might require the storage of metastable *o*-H_2O species for prolonged periods. In an attempt to increase the storage time [25,27], we repeated the experiments described above at a substrate temperature of 8 K and report the spectroscopic OPR for these measurements in Fig. 2(e). A few similarities and striking differences can be clearly seen between these measurements and those obtained at 13 K [Fig. 2(d)].

On the one hand, the magnetically focused beam is characterized by a higher *o*-H_2O content than that of background-deposited water similarly to the enrichment observed for magnetically focused H_2O@Kr at 13 K. Furthermore, expectations of much smaller final OPRs (i.e., OPR < 0.2) and of slower NSC decays [i.e., $k_{\text{eff}} = 0.18(1)\ \text{h}^{-1}$ vs $0.33(3)\ \text{h}^{-1}$ for background-deposited $H_2\ ^{16}O$, and $k_{\text{eff}} = 0.6(1)\ \text{h}^{-1}$ vs $0.62(4)\ \text{h}^{-1}$ for magnetically focused $H_2\ ^{18}O$, at 8 and 13 K, respectively] are indeed borne out. On the other hand, the initial OPR values are much lower than those observed at 13 K for both the magnetically focused beam-deposited and the background-deposited water. Since the sources of the H_2O molecules (magnetically focused beam and background) were identical in both the 8 and the 13 K measurements, the strikingly different initial OPRs provided by the model suggest that the early stages of deposition for H_2O in Kr at 8 K display more complex and rapid NSC dynamics than our simple model can account for. This might also account for the few very large OPR values measured at the very early stages of sample deposition where the signal-to-noise ratio is smallest. These observations suggest that, either directly upon impact with the krypton matrix, or within the initial stage of growth, a significant fraction of impinging water molecules experience rapid NSC. These observations are similar to the behavior described by Sliter *et al.* [29] who recently reported an initial OPR of ~2 for background-deposited $H_2\ ^{16}O$@Ar at 4 K, while observing NSC half-times ~6 h as reported in several previous studies [20,25,28].

Insights leading to better understanding of this behavior may lie in the fact that the rovibrational spectral features of H_2O@Rg are broader and weaker in matrices which were grown at low temperatures. These bands can be made more sharp and intense by a short annealing of the matrix [25], which may result from the fact that matrices grown at low temperatures are more disordered and defective [37]. Further studies will be needed to provide insight into the open questions our measurements raise, namely the existence of a distinctive heterogeneous NSC mechanism [38], the potential role of defects [37], and the existence of a mechanism which leads to different NSC rates for different water isotopes.

In conclusion, magnetic focusing in a supersonic molecular beam provides an efficient separation method yielding a fourfold enrichment in the *o*-H_2O nuclear spin isomer over that of "normal" water. Water samples strongly enriched in *o*-H_2O can now be prepared, isolated, and stored for tens of minutes in Kr at 13 K thereby allowing subsequent manipulations. Attempts to use colder matrices to store the metastable *o*-H_2O species have resulted in a loss of initial enrichment, suggesting the spin dynamics are dependent on the nature and perhaps the structure of the rare-gas film used as a storing media. Access to water samples strongly enriched in *o*-H_2O opens up exciting new perspectives in a wide range of research fields including gas-surface interactions, laboratory astrophysics, spin dynamics in the condensed phase, magnetic resonance spectroscopy, and others.

ACKNOWLEDGMENTS

We thank the NSERC, CQMF, ISF (Grant No. 2011185), RBNI-Nevet program, and the Taub Foundation's Landau fellowship for financial support. Enlightening discussions with Dr. Patrice Cacciani, Dr. Xavier Michaut, and Professor Emil Polturak are gratefully acknowledged, as well as Professor Yael Dubowski for kindly lending us a D316 detector.

[1] W. Heisenberg, Z. Phys. **41**, 239 (1927).
[2] F. Hund, Z. Phys. **42**, 93 (1927).
[3] D. M. Dennison, Proc. R. Soc. London, Ser. A **115**, 483 (1927).
[4] K. F. Bonhoeffer and P. Harteck, Naturwissenschaften **17**, 182 (1929).
[5] A. Farkas, *Orthohydrogen, Parahydrogen, and Heavy Hydrogen* (Cambridge University Press, Cambridge, UK, 1935).
[6] P. L. Chapowsky and L. J. F. Hermans, Annu. Rev. Phys. Chem. **50**, 315 (1999).
[7] Z.-D. Sun, K. Takagi, and F. Matsushima, Science **310**, 1938 (2005).
[8] E. Gershnabel and I. S. Averbukh, Phys. Rev. A **78**, 063416 (2008).
[9] G. Peters and B. Schramm, Chem. Phys. Lett. **302**, 181 (1999).

[10] J. Küpper, F. Filsinger, and G. Meijer, Faraday Discuss. **142**, 155 (2009).
[11] M. J. Mumma, H. A. Weaver, H. P. Larson, D. S. Davis, and M. Williams, Science **232**, 1523 (1986).
[12] M. R. Hogerheijde, E. A. Bergin, C. Brinch, L. I. Cleeves, J. K. J. Fogel, G. A. Blake, C. Dominik, D. C. Lis, G. Melnick, D. Neufeld, O. Panić, J. C. Pearson, L. Kristensen, U. A. Yıldız, and E. F. van Dishoeck, Science **334**, 338 (2011).
[13] C. R. Bowers and D. P. Weitekamp, Phys. Rev. Lett. **57**, 2645 (1986).
[14] V. I. Tikhonov and A. A. Volkov, Science **296**, 5577 (2002).
[15] S. L. Veber, E. G. Bagryanskaya, and P. L. Chapovsky, Pis'ma Zh. Éksp. Teor. Fiz. **129**, 86 (2006) [JETP Lett. **102**, 76 (2006)].
[16] P. Cacciani, J. Cosléou, and M. Khelkhal, Phys. Rev. A **85**, 012521 (2012).
[17] H.-H. Limbach, G. Buntkowsky, J. Matthes, S. Gründemann, T. Pery, B. Walaszek, and B. Chaudret, Chem. Phys. Chem. **7**, 551 (2006).
[18] G. Buntkowsky, H.-H. Limbach, B. Wlalaszek, A. Adamczyk, Y. Xu, H. Breitzke, A. Schweitzer, T. Gutmann, M. Wächtler, J. Frydel, T. Emmler, N. Amadeu, D. Tietze, and B. Chaudret, Z. Phys. Chem. **222**, 1049 (2008).
[19] T. Kravchuk, M. Reznikov, P. Tichonov, N. Avidor, Y. Meir, A. Bekkerman, and G. Alexandrowicz, Science **331**, 319 (2011).
[20] R. F. Curl, J. V. V. Kasper, and K. S. Pitzer, J. Chem. Phys. **46**, 3220 (1967).
[21] R. L. Redington and D. E. Milligan, J. Chem. Phys. **39**, 1276 (1963).
[22] G. P. Ayers and A. D. E. Pullins, Spectrochim. Acta **32**, 1689 (1976).
[23] D. Forney, M. E. Jacox, and W. E. Thompson, J. Mol. Spectrosc. **157**, 479 (1993).
[24] J. P. Perchard, Chem. Phys. Lett. **273**, 217 (2001).
[25] C. Pardanaud, Ph.D. thesis, Université Pierre et Marie Curie—Paris VI, Paris, 2007, p. 253.
[26] C. Pardanaud, A.-M. Vasserot, X. Michaut, and L. Abouaf-Marguin, J. Mol. Struct. **873**, 181 (2008).
[27] L. Abouaf-Marguin, A.-M. Vasserot, C. Pardanaud, and X. Michaut, Chem. Phys. Lett. **480**, 82 (2009).
[28] X. Michaut, A.-M. Vasserot, and L. Abouaf-Marguin, Vib. Spectrosc. **34**, 83 (2004).
[29] R. Sliter, M. Gish, and A. F. Vilesov, J. Phys. Chem. A **115**, 9682 (2011).
[30] C. Manca-Tanner, D. Schmidiger, and M. Quack, Faraday Discuss. **150**, 113 (2011).
[31] W. B. Chapman, A. Kulcke, B. W. Blackmon, and D. J. Nesbitt, J. Chem. Phys. **110**, 8543 (1999).
[32] A. P. Jardine, P. Fouquet, J. Ellis, and W. Allison, Rev. Sci. Instrum. **72**, 3834 (2001).
[33] J. Tennyson *et al.*, J. Quant. Spectrosc. Radiat. Transfer **110**, 573 (2009).
[34] R. A. Toth, J. Opt. Soc. Am. B **9**, 462 (1992).
[35] L. Lodi and J. Tennyson, J. Quant. Spectrosc. Radiat. Transfer **113**, 850 (2012).
[36] For magnetically focused molecular beam-deposited $H_2{}^{18}O$ having an ortho:para ratio of OPR_b, $J_b OPR_b/(OPR_b+1)$–$d[o\text{-}H_2{}^{18}O]/dt = d[p\text{-}H_2{}^{18}O]/dt - J_b/(OPR_b+1) = k_{o\to p}[o\text{-}H_2{}^{18}O] - k_{p\to o}[p\text{-}H_2{}^{18}O]$ where J_b is the beam deposition rate of $H_2{}^{18}O$. Identical expressions describe the coupled growth and conversion kinetics in background-deposited $H_2{}^{16}O$, but use the corresponding values for the deposition rate, J_B, and ortho:para ratio, OPR_B.
[37] W. Langel, W. Schuller, E. Knözinger, H. W. Fleger, and H. J. Lauter, J. Chem. Phys. **89**, 1741 (1988).
[38] M. Tudorie, M. Khelkhal, J. Cosléou, and P. Cacciani, Surf. Sci. **601**, 1630 (2007).